

# UC Irvine

## UC Irvine Previously Published Works

### Title

Enterovirus Persistence in Cardiac Cells of Patients With Idiopathic Dilated Cardiomyopathy Is Linked to 5 Terminal Genomic RNA-Deleted Viral Populations With Viral-Encoded Proteinase Activities.

### Permalink

<https://escholarship.org/uc/item/0nn0q5tx>

### Journal

Circulation, 139(20)

### Authors

Bouin, Alexis  
Gretteau, Paul-Antoine  
Wehbe, Michel  
[et al.](#)

### Publication Date

2019-05-14

### DOI

10.1161/CIRCULATIONAHA.118.035966

Peer reviewed



Published in final edited form as:

*Circulation*. 2019 May 14; 139(20): 2326–2338. doi:10.1161/CIRCULATIONAHA.118.035966.

## Enterovirus persistence in cardiac cells of patients suffering from idiopathic dilated cardiomyopathy is linked to 5' terminal genomic RNA-deleted viral populations with viral-encoded proteinase activities

Alexis Bouin, PhD<sup>1,2,\*</sup>, Paul-Antoine Gretteau, PhD<sup>1,\*</sup>, Michel Wehbe, PhD<sup>1,3,\*</sup>, Fanny Renois, PhD<sup>1,4,5</sup>, Yohan N'Guyen, MD<sup>1,5</sup>, Nicolas Leveque, MD PhD<sup>1,5,6</sup>, Michelle N. Vu, BS<sup>2</sup>, Steven Tracy, PhD<sup>7</sup>, Nora M. Chapman, PhD<sup>7</sup>, Patrick Bruneval, MD PhD<sup>8</sup>, Paul Fornes, MD PhD<sup>1,5</sup>, Bert L. Semler, PhD<sup>2,\*\*</sup>, and Laurent Andreoletti, MD PhD<sup>\*\*1,5</sup>

<sup>1</sup>EA-4684 Cardiovir, Faculty of Medicine, University of Reims Champagne-Ardenne (URCA), Reims, France

<sup>2</sup>Department of Microbiology and Molecular Genetics, School of Medicine, University of California, Irvine, CA, USA

<sup>3</sup>Centre AZM pour la recherche en biotechnologie et ses applications, Université Libanaise, Tripoli, Lebanon

<sup>4</sup>LUNAM University, Oniris, LABERCA, UMR INRA 1329, 44307, Nantes, France

<sup>5</sup>CHU Robert Debré, Laboratoire de Virologie Médicale et Moléculaire, Reims, France

<sup>6</sup>EA-4331 LITEC, Faculty of Medicine and Pharmacy, University Hospital of Poitiers, Poitiers, France

<sup>7</sup>Department of Pathology and Microbiology, University of Nebraska Medical Center, Omaha, NE, USA

<sup>8</sup>Service d'Anatomie Pathologique, Hôpital Européen Georges Pompidou, Paris, France

### Abstract

**1. Background:** Group B enteroviruses are common causes of acute myocarditis which can be a precursor of chronic myocarditis and dilated cardiomyopathy (DCM), leading causes of heart transplantation. To date, the specific viral functions involved in the development of DCM remain unclear.

**\*\*Correspondence:** Laurent Andreoletti, Laboratoire de Virologie médicale et moléculaire, et EA-4684 Cardiovir, Hôpital Robert Debré, Avenue du Général Koenig, 51092 REIMS Cedex, France. Tel: (+33) 3 26 78 77 02; Fax: (+33) 3 26 78 41 34; landreoletti@chu-reims.fr; Bert L. Semler, Department of Microbiology and Molecular Genetics, School of Medicine, University of California, Irvine, CA, 92697 USA; Tel: (+1) 949-824-7573; Fax (+1) 949-824-8598; blsemler@uci.edu.  
\* contributed equally

#### Disclosure

None of the authors of the present manuscript have a commercial or other association that might pose a conflict of interest (*e.g.*, pharmaceutical stock ownership, consultancy).

**2. Methods:** Total RNA from cardiac tissue of patients suffering from DCM was extracted, and sequences corresponding to the 5' termini of enterovirus RNAs were identified. Following NexGen RNA sequencing, viral cDNA clones mimicking the enterovirus RNA sequences found in patient tissues were generated *in vitro*, and their replication and impact on host cell functions were assessed on primary human cardiac cells in culture.

**3. Results:** Major enterovirus B populations characterized by 5' terminal genomic RNA deletions ranging from 17 to 50 nucleotides were identified either alone or associated with low proportions of intact 5' genomic termini. *In situ* hybridization and immuno-histological assays detected these persistent genomes in clusters of cardiomyocytes. Transfection of viral RNA into primary human cardiomyocytes demonstrated that deleted forms of genomic RNAs displayed early replication activities in the absence of detectable viral plaque formation, whereas mixed deleted and complete forms generated particles capable of inducing cytopathic effects at levels distinct from those observed with full-length forms alone. Moreover, deleted or full-length and mixed forms of viral RNA were capable of directing translation and production of proteolytically active viral 2A<sup>pro</sup> in human cardiomyocytes.

**4. Conclusion:** We demonstrate that persistent viral forms are composed of B-type enteroviruses harboring a 5' terminal deletion in their genomic RNAs and that these viruses alone or associated with full-length populations of helper RNAs could impair cardiomyocyte functions by the proteolytic activity of viral 2A<sup>pro</sup> in unexplained DCM cases. These results provide a better understanding of the molecular mechanisms that underlie the persistence of EV forms in human cardiac tissues and should stimulate the development of new therapeutic strategies based on specific inhibitors of the CV-B 2A<sup>pro</sup> activity for acute and chronic cardiac infections.

### Keywords

Enterovirus; dilated cardiomyopathy; 5' terminal genomic deletion; persistent infection; viral 2A<sup>pro</sup>

---

### Introduction

Enteroviruses (EVs) are small, single-stranded, positive-sense RNA viruses with genomes of approximately 7,400 nucleotides. The genome is flanked on both ends by untranslated regions (UTRs) (Figure 1A). The 5' UTR is crucial for initiating the replication and translation of the viral genome<sup>1</sup>. Enteroviruses are common human pathogens, although the majority of EV infections are asymptomatic, these viruses, especially the six serotypes of group B coxsackieviruses (CV-B1 through CV-B6), are a common cause of acute myocarditis in children and young adults. Myocarditis can progress in 10–20% of cases to chronic myocarditis and subsequently to dilated cardiomyopathy (DCM, prevalence = 7 cases / 100,000; second leading cause of heart transplantation worldwide)<sup>2</sup>. The concept that endomyocardial persistent EV infection is the etiological cause of a subset of idiopathic DCM cases is supported by the detection of EV genomes and enteroviral capsid protein VP1 in as many as 35% of explanted heart tissues from end-stage DCM patients<sup>3,4</sup>. However, the molecular mechanisms by which EVs cause both human myocarditis and progression to DCM remain poorly understood, a barrier which limits the development of specific therapeutic strategies against EV-induced chronic heart diseases.

In 2008, Chapman and co-workers reported the characterization of a CV-B2 infection by a virus harboring a 5' terminal deletion (TD) in cardiac muscle tissues collected from a human fatal fulminant myocarditis case<sup>5</sup>. Transfection of 5' terminally deleted CV-B3 synthetic RNA into HeLa cells generated non-cytolytic virus (CV-B3/TD). Similar results have been observed in murine cardiomyocytes and in murine models<sup>6</sup>. These TD populations were studied in persistent murine cardiac infections and characterized by low ratios of positive to negative [(+)/(-)] RNA strands, a low production of infectious particles, and low viral protein synthesis activities<sup>5,6</sup>. RNA sequencing revealed CV-B TD populations harboring 5' terminal genomic deletions ranging in size from 8 to 49 nucleotides. The genomic deletions involved the loss of the 5' terminal sequences making up the 5' half of stem "a," all or part of stem-loops "b" and "c" of the predicted cloverleaf-like RNA secondary structure (also known as stem-loop I; refer to Figure 1B) but leaving the stem-loop "d" domain intact. Stem-loop "d" contains a binding site for the viral 3CD protein, an RNA polymerase precursor required for viral genomic RNA replication (Figure 1B)<sup>7</sup>. Recent work has shown that although 5' terminal deletions through the stem-loop "d" region still allow replication, the inability to detect these in naturally occurring TD virus populations suggests that either the presence of stem-loop "d" may be necessary in most naturally-occurring infections or that such deletions are quite rare<sup>8</sup>.

In 2016, a mixture of 5' terminally-deleted and full-length coxsackievirus B3 (CV-B3) RNA populations in heart biopsies of an unexplained dilated cardiomyopathy case induced by a persistent enterovirus infection was identified<sup>9</sup>. The deleted forms were the major species of RNA, with the full-length forms being the minor RNA species in these samples. These results suggested that the 5' TD populations, which were associated with a minor full-length virus population, could potentially be involved in persistence in human cardiac tissue via genomic interactions<sup>10,11</sup>, even if TD viruses can replicate on their own<sup>5,6,8</sup>. The evolution of TD populations during the myocarditis phase may explain how the virus can persist in the heart long after the acute infection, subsequently leading to the development of chronic myocarditis and DCM; however, further molecular investigation on a larger number of cardiac tissues of unexplained DCM adult patients is necessary to adequately test the hypothesis that the association of major TD and minor full-length viral RNA populations is common in persistent viral infections. Moreover, the concept that persistent, low-efficiency replication of EV-B deleted and full-length genomic RNA combined populations could contribute together to the development of cardiac viral persistence, and subsequently to the pathogenesis of unexplained DCM cases, remains to be investigated.

Previous reports described the effect of enterovirus persistent infection in cardiac tissue. Enterovirus proteinase 2A (2A<sup>pro</sup>) has been shown to cleave dystrophin in cardiomyocytes of infected mice<sup>12</sup>. It was later shown that the expression of 2A<sup>pro</sup> alone is sufficient to induce DCM in a murine model<sup>13</sup>. Finally, it has been shown in a murine model that if more than 50% of the membrane bound dystrophin was disrupted by 2A<sup>pro</sup> in cardiac tissue, mice were more likely to develop cardiomyopathy, and that the presence of the C-terminal cleavage fragment of dystrophin was more harmful than a complete lack of the protein<sup>14</sup>.

In the present study, we performed a comprehensive molecular analysis using a next generation sequencing (NGS) strategy of the 5' terminal genomic RNAs of persistent EV

populations detected in explanted heart tissue samples from patients with unexplained end-stage DCM with persistent EV-B infections. Subsequently, synthetic CV-B3 RNAs harboring 5' terminal deletions like those observed in persistent viral populations were generated *in vitro* and transfected into cultured human primary cardiomyocytes. This cellular model allowed us to investigate viral replication and translation activities of deleted viral RNA forms alone or in association with the full-length viral RNA form in cardiomyocytes. Our results revealed mechanistic insights into how these forms of viral RNA could potentiate the development of DCM in humans.

## Materials and Methods

The data, analytic methods, and study materials will not be made available to other researchers for purposes of reproducing the results or replicating the procedure, because the human biological samples (cardiac tissues) as well as RNA extracted from human primary cardiomyocytes used in our experiments remain limited biological sources.

A further detailed version of materials and methods is provided as supplementary data.

### Human cardiac tissue samples

Explanted endomyocardial tissue samples (n = 119) were obtained from 24 adult patients with idiopathic dilated cardiomyopathy (IDCM) according to the classification of cardiomyopathies by the Heart Failure Association of the European Society of Cardiology (ESC report)<sup>15</sup>.

The control group, collected from 14 adult patients without past medical history of cardiac pathology and macroscopic or microscopic cardiac tissue abnormalities and who died from suicides or traumatic accidents, was retrospectively selected.

The institutional review committee (HEGP, Paris, France) approved the study and informed consent was obtained from the patients or subjects' families at the time of heart transplantation. Our investigations conformed to the principles outlined in the Declaration of Helsinki for use of human tissue or subjects.

### RNA and DNA extraction from cardiac tissue

Nucleic acids were extracted from formalin fixed and paraffin embedded (FFPE) tissue blocks. Briefly, samples were dewaxed and digested in proteinase K. Total nucleic acid (DNA and RNA) extractions were performed from tissue sample lysates using a NucliSens easyMAG device (BioMerieux).

### Genomic detection of common human cardiotropic viruses in explanted cardiac tissues of IDCM patients

To detect enteroviruses (EV) and to rule out the presence of all human herpesviruses, we employed PCR assays coupled to microarray hybridization analyses (Clart Entherpex V8.0). To rule out human parvovirus B19 (PV-B19) infections, we used a specific real-time PCR assay (Argene Biomerieux)<sup>16</sup>.

### **Specific detection of viral RNA and calculation of RNA(+)/RNA(-) ratios in human cardiac tissues and infected cultured cells**

Reverse transcription was carried out using Superscript II reverse transcriptase (Invitrogen). Quantitative PCR was performed using iQ™ Supermix (BioRad) to specifically detect total and negative-strand RNA. Positive-strand RNA copy number was calculated by subtracting the number of negative strands from total number of RNA strands, and the [(+)/(-)] ratio was determined by dividing the calculated number of positive RNA strands by the number of negative-strand RNAs detected (Supplemental Table 1).

### **Next generation sequencing strategies for enterovirus detection and molecular characterization**

Total nucleic acids extracted from FFPE samples were used to generate NGS libraries as described previously<sup>9</sup>. Sequence reads were analyzed using CLC Genomics (CLC Bio). Sequences were aligned against the CV-B3 Nancy reference genome (Genbank accession number: M88483.1). Coverage data were used to assess the presence of terminal deletions in the viral genome (Supplemental Table 1).

### **Analysis of coverage data for deletion detection and population estimates**

Alignment of the reads against the CV-B3 Nancy genome generated coverage values for each nucleotide position near the 5' terminus. These data were used to identify deletions. The strategies described for frozen samples in our previous work have been applied in the present study<sup>9</sup>, within the limits of occurrence of random disruption of the genome during FFPE sample processing<sup>17</sup>.

### **Viruses and cDNA cloning approaches of persistent viral RNA forms**

The origin of the coxsackievirus B3/28 (cardiovirulent strain) plasmid used in this study has been previously described<sup>18</sup> (Supplemental Table 1). The TD viral RNAs were synthesized using a MEGAscript™ T7 Transcription Kit (Invitrogen) and purified using a MEGAclean™ Transcription Clean-Up Kit (Invitrogen).

### **Cell culture**

HeLa cells were grown in minimal Eagle's essential medium (MEM, Life Technologies) supplemented with 10% fetal bovine serum (FBS, Life Technologies), 2 mM L-glutamine (Life Technologies), and 1% penicillin/streptomycin (Life Technologies). Human primary cardiomyocytes (HCM, ScienCell Research Laboratories), were cultured in cardiac myocyte medium (ScienCell Research Laboratories) supplemented with 5% FBS (ScienCell Research Laboratories) in tissue culture flasks coated with poly-L-lysine (ScienCell Research Laboratories). Cardiac myocyte cell cultures were passaged twice a week, and the cells were used between passages 4 to 14.

To test the effect of inhibitors on replication or eIF4G cleavage, compounds were added to cell culture. 2A proteinase inhibitor Z-VAD-FMK (UBPBio) was added at a concentration of 50 μM, and a portion of the media was changed every 6 hr for 24 hr<sup>19</sup>. As Z-VAD-FMK was initially used as a pan-caspase inhibitor, and caspase-3 was previously reported to

disrupt eIF4G<sup>20</sup>, we designed a replicon harboring a catalytically inactive 2A proteinase (C107S) similar to the work of Yu *et al.*<sup>21</sup>. To verify inhibition of viral RNA replication, transfections (as described below) were carried out in the presence or absence of 2 mM guanidine hydrochloride (GuHCl) and 8  $\mu$ M fluoxetine (F)<sup>22,23</sup>.

### Transfection

After trypsinization, cells (HCM or HeLa) were seeded in 24-well plates (Nunclon delta surface, Thermo Scientific). Plates were incubated at 37°C for the indicated times. The supernatants were collected and the cells washed twice with DPBS.

### Viral RNA detection by *in situ* hybridization assay in human cardiac tissues

To detect endomyocardial viral RNA, *in situ* hybridization (ISH) was performed using QuantiGene® ViewRNA ISH FFPE Tissue Assay (Panomics Affymetrix). Cardiac sections (4  $\mu$ m) were cut and mounted on Superfrost® slides (ThermoFisher Scientific). The slides were then treated as recommended by the manufacturer's protocol (Panomics Affymetrix).

### Viral RNA and virus production in HCM culture

Viral RNA in culture supernatant and in HCM cells was extracted from the lysate using QIAamp Viral RNA Kit (Qiagen). Viral RNA copy number in transfected HCM was quantitated by RT-qPCR using a StepOne plus real time PCR system (ThermoFisher Scientific) by a method similar to that described previously<sup>24</sup>.

Plaque assays were used to detect infectious particles in culture supernatants and in HCM cells.

### *In vitro* translation analysis

To assess viral protein synthesis, an *in vitro* translation assay was carried out by incorporating <sup>35</sup>S-methionine into newly-synthesized proteins as previously described<sup>25,26</sup>. The samples were subjected to electrophoresis in SDS-containing Tris-glycine buffer on a polyacrylamide gel. The gel was exposed to X-ray film overnight prior to developing using a phosphorimager.

### Viral protein production and detection of 2A<sup>Pro</sup> activity

HCM were transfected with indicated quantities of viral RNA using TransIt reagent (Mirus Bio) and incubated for 24 hr at 37°C. To mimic the proportions of terminally deleted to full-length viral RNA observed in patients' cardiac tissues, a ratio of 19:1 was used. A Western blot using antibodies targeting enterovirus VP1 (Dako, anti-enterovirus clone5-D8/1), GAPDH (ab181602, Abcam), Caspase-3 (Abcam, ab13585) or eIF4G (Cell signaling, #2469) was performed.

### Statistics

Quantitative variables were all compared using the Mann Whitney U test and a p-value < 0.05 was considered statistically significant. To assess the inhibition effect of guanidine hydrochloride/Fluoxetine on the viral replication, we performed repeated measures two-way



ANOVA test. All statistical analyses were performed using GraphPad Prism 7 (GraphPad) and SAS version 9.4 (SAS Institute Inc.).

## Results

### Identification of persistent endomyocardial enterovirus infections in unexplained IDCM cases.

The presence of EV RNA was detected by RT-qPCR in 8 (33%) of 24 IDCM patients, whereas none of the 14 control patients were positive for EV RNA detection in cardiac tissues (Figure 2A). The presence of borderline myocarditis according to the Dallas criteria was detected in 2 EV positive IDCM patients and 2 EV negative IDCM patients. PCR assays for the detection of other common cardiotropic viruses were negative for human herpesviruses 1–8 in the entire cohort. Parvovirus B19 (PV-B19) genomic DNA was detected in 62.5% of these EV positive IDCM patients (data not shown). PVB19 infection displayed normalized viral loads lower than 500 copies per  $\mu\text{g}$  of nucleic acid extracted, below the clinical threshold previously defined by Bock *et al.*<sup>27</sup>, ruling out this virus as a source of pathogenesis in these patients (data not shown). To detect and quantify EV RNA in explanted cardiac tissues of patients suffering from IDCM at the stage of heart transplantation, we performed a standardized one-step real-time RT-PCR assay targeting the 5' UTR of the EV genome<sup>28</sup>. The standardized median viral load value in IDCM patient cardiac tissues was estimated at  $5.4 \times 10^4$  copies (range:  $3.4 \times 10^3 - 3.7 \times 10^6$ ) per microgram of total extracted nucleic acids (Figure 2A). No significant differences were observed between viral load values obtained from left ventricle, right ventricle, or septum taken from the same patients (Figure 2A). EV negative and positive RNA strands were quantified using specific RT-qPCR, producing [(+)/(-)] EV RNA ratios ranging from 1.06 to 5.28 (mean value = 2.65) (Figure 2B). Standard acute EV infections typically show [(+)/(-)] RNA ratios between 30:1–100:1<sup>29,30</sup>, suggesting that the [(+)/(-)] ratios in these clinical samples were aberrant. As expected from previous studies<sup>28</sup>, a positive correlation between total viral load and [(+)/(-)] EV RNA ratio values was observed in cardiac tissues of DCM patients ( $R^2=0.70$ ;  $P=0.039$ ; Figure 2C). ISH assays showed that viral RNA was detectable in cardiomyocytes (Figure 2D). The infected cells were distributed in clusters, highlighted by a large variability of ISH signal between several areas of the same sample (Figure 2E). Using serial slides of cardiac samples, a co-localization between viral RNA, viral protein, and dystrophin disruption was observed (Figure S1) These findings indicate that the eight EV-positive DCM patients displayed the hallmarks of a persistent EV infection, characterized by low EV RNA load, [(+)/(-)] EV RNA ratio values near or below 5.0 (Figure 2). Therefore, these patients will be referred as EV-DCM.

### Molecular characterization of 5' terminal RNA deletions present in persistent EV-B populations using a next generation sequencing strategy

The 5' terminal regions of EV RNAs isolated from persistent infections were characterized using a previously developed and validated NGS strategy<sup>9</sup>. Sequence analyses allowed us to identify high nucleotide identity rates (>85%) with 5' UTR CVB-3 and EV Group-B (EV-B) RNA genomes (not shown). Interestingly, the persistent EV-B strains harbored 5' terminal deletions ranging in size from 17 to 50 nucleotides. These mutations had deleted part or all



cloverleaf stem “a” and stem-loops “b,” “c,” and “d” (Figure 3C and Supplemental Figure 2). The viral variants were classified in 3 different groups: full-length 5' UTR (FL), deletion of the 5' terminal 17 to 36 nucleotides (17–36), and deletion of the 5' terminal 37 to 50 nucleotides (37–50). Each sample displayed a similar pattern of deletions (Figure 3A). Viral genomes containing partially deleted 5' UTRs as well as low levels of full-length viral RNA populations were detected in all patients (Figure 3A). Considering the entire cohort, the group with 5' terminal deletions ranging from 37–50 nucleotides represented the major population of viruses detected (>79%) (Figure 3B,  $P < 0.0001$ ). Moreover, a negative correlation was observed between EV total RNA levels and the proportion of deleted viral forms identified in heart samples (Figure 3D,  $R^2 = 0.54$ ;  $P = 0.016$ ). These findings indicated that the endomyocardial EV persistent genomes were composed of major populations of 5' UTR terminally deleted RNAs that can be separated into two groups based on the extent of RNA deletions. In addition, each of these populations was associated with a minor population of full-length 5' UTR -containing EV genomes.

### Genome replication of persistent EV-B viral RNA populations in human cardiomyocytes

Undeleted (FL) and 50 nt deleted (d50) CV-B3/28 genomic RNAs were cloned and *in vitro* transcribed. To assess early and late replication activities of persistent CV-B3/28 RNA populations in primary human cardiac cells, CV-B3/28-FL and CV-B3/28-d50 RNAs were transfected in cells alone or together. Total viral RNA (positive- and negative-strands), negative-strand RNA, and plaque production levels were assessed until 48 hr post transfection in human primary cardiomyocytes (HCM) (Figure 4). Analysis of total viral RNA levels demonstrated that CV-B3/28-d50 RNA forms displayed an absence of viral genome amplification in HCM at 8 hr post-transfection (Figure 4A), whereas full-length forms and mixed forms (ratio of 19:1, deleted RNA:full-length RNA) produced significantly higher viral RNA replication activities than those observed with the d50 form alone at 24 hr post-transfection ( $P < 0.05$ ; Figure 4A). Interestingly, mixed forms produced significantly lower viral RNA replication activities than those observed with the complete form alone at 48 hr post-transfection ( $P < 0.05$ ; Figure 4A). This absence of RNA amplification for deleted forms was subsequently associated with a defect in positive-strand viral RNA synthesis levels at 24 hr post-transfection, as demonstrated by our RNA [(+)/(–)] strand ratio analyses (RNA ratio values at 12 hr vs. 24 hr:  $P < 0.01$ ; Figure 4B). RNA strand ratios are somewhat skewed at the earliest time points, likely due to the presence of high levels of transfected positive-strand RNA, particularly in transfections of the d50 in which very low levels of RNA replication occur. This could, in part, explain the [(+)/(–)] strand ratio obtained for mixed RNA forms at 24 hr that was followed by a significant decrease of the [(+)/(–)] RNA ratio at 48 hr post-transfection (RNA ratio values at 24 hr vs. 48 hr:  $P < 0.01$ ; Figure 4B).

To analyze the early replication activities of full-length, deleted, and mixed viral RNA forms in HCM, a viral RNA replication inhibition assay using a combination of fluoxetine and guanidine hydrochloride (two inhibitors of viral RNA replication that act on viral protein 2C) was performed at 0, 2, and 8 hr post-transfection for each viral RNA form (Figure 4C). Deleted and mixed forms produced RNA between 0 and 8 hr post-transfection, and RNA synthesis was inhibited by the fluoxetine and guanidine hydrochloride mixture (GuHCl/F; CV-B3-FL:  $P = 0.005$ ; CV-B3/28-d50:  $P = 0.005$ ; CV-B3/28-d50 and CV-B3/28-FL forms:

P=0.04; Figure 4C). Positive strand RNA copy numbers of deleted and mixed forms decline in the absence of RNA replication but remain somewhat stable when replication is not inhibited, demonstrating that low-level RNA synthesis is capable of maintaining a stable population of genomic RNAs in the cell. Under these same conditions, full-length RNA forms displayed an amplification of genome explained by a much greater level of viral RNA synthesis (Figure 4C, left panel). The production of virus detectable by plaque assays (*i.e.*, wild type virus) from the transfected mixed forms was slightly higher at 24 hr post-transfection but significantly lower at 48 hr post-transfection compared to yields for the full-length form alone at 24 and 48 hr post-transfection, respectively (24 hr: P<0.05; 48 hr: P<0.05; Figure 4D). No plaques were detected in HCM transfected with the d50 form alone (Figure 4D). These assays confirmed the viral RNA replication levels observed in Figure 4A. Moreover, they were compatible with the significant variations of EV RNA ratios depicted in Figure 4B at 48 hr. Such variations may, in part, be due to interference by the d50 form with replication of the full-length form of viral RNAs or by a strand-specific defect in viral RNA synthesis directed by the deleted forms of CV-B3 RNA.

### Effect of viral protein production by 5' terminally-deleted EV-B RNAs on the host cell

Since the deleted forms of EV-B genomic RNAs displayed reduced RNA synthesis capabilities, a key biological issue was to determine if these deleted forms are capable of producing pathological effects on infected cells and tissues. As a first step in addressing this question, we assessed the translation efficiency of the deleted forms of CV-B genomic RNAs. *In vitro* translation assays were performed on full-length RNAs as well as RNAs with 5' terminal deletions of 50 nt and 100 nt, the latter of which removed all of the RNA sequences of the 5' cloverleaf structure (Figure 1B). There were no significant differences in the translation profiles among these three viral RNA forms (Figure S3).

To further determine the possible effects of persistent EV-B protein production in infected cardiomyocytes, Western blot analysis was performed on HCM at 24 hr post-transfection. To mimic the proportion of 5' terminally deleted to full-length viral genomes (1:19) observed in patients' cardiac tissue, we transfected 125 ng of full-length RNA and 2,375 ng of d50 RNA alone or in combination (Figure 5A). The viral 2A<sup>pro</sup> is responsible for cleavage of dystrophin in cardiac tissue<sup>12</sup>. However, because dystrophin is a very large protein and difficult to detect by Western blot, we targeted the 2A proteinase activity by monitoring the status of eukaryotic translation initiation factor 4G (eIF4G) in the above-described protein extracts. Enterovirus proteinase 2A is known to cleave eIF4G as part of the viral shut off host protein synthesis<sup>31,32</sup>. We used Western blot analysis to detect eIF4G and its cleavage products as a measure of enterovirus 2A<sup>pro</sup> activity and thus, as a surrogate for dystrophin cleavage. Significantly, the samples transfected with viral RNA displayed a readily-detectable cleavage fragment of eIF4G1 with signal reaching 0.73, 1.07, and 1.23 when normalized to GAPDH signal for FL, d50, and mixed forms, respectively, highlighting the high-level activity of 2A<sup>pro</sup> even in samples transfected with deleted genomes only (Figure 5A, lanes 2–4; quantified in Figure 5B, columns 2–4). An inhibitor of CV-B3 2A<sup>pro</sup>, Z-VAD-FMK, was used to confirm the involvement of this viral protein in the cleavage process, resulting in the near complete inhibition of cleavage of eIF4G (Figure 5D). As caspase-3 activation has been shown to result in the cleavage of eIF4G<sup>20</sup>, and Z-VAD-FMK

is a pan-caspase inhibitor, we checked for caspase-3 activation in human cardiomyocytes (Figure 5E) and could not detect active caspase signal in either full-length or deleted RNA transfection. To fully validate that the eIF4G disruption was caused by 2A<sup>Pro</sup>, we transfected a full-length RNA encoding an inactive 2A proteinase (Figure 5F). The presence of an inactive form of 2A proteinase abolished eIF4G cleavage.

In addition to monitoring 2A proteinase activity via eIF4G cleavage in transfected cells, we also analyzed the synthesis of viral protein VP1. Unlike the VP1 production we detected in *in vitro* translation assays (Figure S3), we were unable to detect this protein by Western blot analysis following transfection of CV-B3/28 RNA harboring a 50 nt 5' terminal deletion (Figure 5A, lane 3). In contrast, the full-length RNA form produced significant levels of viral protein VP1 (Figure 5A, lane 2). When full-length RNA was transfected in combination with genomic RNA harboring a 50 nt 5' terminal RNA deletion, significantly reduced levels of VP1 were detected (Figure 5A, lane 4; quantified in Figure 5C, P<0.05).

Given that the initial data (shown in Figure 5A) were generated by transfecting fixed amounts of viral RNA, an additional experiment was carried out to determine if the production of eIF4G cleavage products and viral protein VP1 in transfected cardiomyocytes occurred in a dose-dependent manner (Figure 5G). Transfection of the full-length form of CV-B3 RNA produced detectable cleavage of eIF4G at the lowest amount of viral RNA used (250 ng), with the levels of cleavage products (CP) increasing when increasing amounts of viral RNA were used. Transfection of the d50 form of RNA also produced eIF4G cleavage products in a dose-dependent manner, albeit at lower levels than those observed for full-length RNAs (Figure 5G). Likewise, VP1 production could be detected in a dose dependent manner for the full-length form of CV-B RNA, but not for the deleted form, as previously observed (Figure 5A).

## Discussion

Enterovirus (EV) infections have been strongly implicated in chronic human diseases such as diabetes<sup>33</sup>, chronic myocarditis, and dilated cardiomyopathy (DCM)<sup>34–36</sup>. During the last 20 years, the involvement of coxsackievirus B (CV-B) persistent infection in chronic myocarditis leading to the development of DCM has been supported by the detection of EV-B viral genomic RNA replication and translation activities in explanted heart tissues of a subset of patients at the end-stage of unexplained DCM<sup>3,37,38</sup>. An ongoing persistent viral infection could explain how chronic cardiomyopathies develop via the continuous synthesis of viral proteins with pro-apoptotic, immuno-modulating, and disruptive activities for cellular structures and functions<sup>39</sup>. However, the exact mechanisms of viral persistence in human cardiac tissues are largely unknown, thereby limiting development of specific therapeutic strategies. Deletions in the 5' terminus of CV-B genomic RNAs have been documented<sup>5,6</sup>, leading to the generation of so-called TD viruses. Given that TD viruses have a very restricted replicative capacity compared to full-length CV-B, the generation and/or maintenance of such variants could be a process that allows EV to persist in the heart long after the acute infection<sup>2</sup>. These deleted forms were reported for the first time in a patient suffering from fulminant myocarditis<sup>5</sup>. More recently, terminally-deleted forms of viral RNA were reported in a case of persistent CV-B3 infection associated with unexplained

DCM<sup>9</sup>, but the putative role of TD viral RNAs in cardiac pathogenesis required a comprehensive study in a larger cohort of affected patients.

In the present investigation, we detected EV-B RNA in 33% (8/24) of explanted heart tissues of an original, end-stage cohort of patients suffering from unexplained DCM. The infection was characterized by a low average viral load and by low [(+)/(-)] strand ratios (*i.e.*, below 5), previously described for persistent infections in EV-induced DCM murine models<sup>6</sup> or in EV-related human pathologies such as chronic fatigue syndrome<sup>40</sup>. Moreover, previous studies reported that deleted viruses in culture produced similar amount of positive and negative RNAs, leading to a ratio of close to 1<sup>5</sup>. It should be noted that full-length EV-infected cells express much higher ratios of positive- to negative-strand viral RNAs, ranging between 30:1 and 100:1<sup>29,30,41</sup>. Interestingly, we observed a significant positive correlation between viral load and the [(+)/(-)] ratio, indicating that decreased viral load was associated with a smaller proportion of positive-strand RNA and suggesting that the persistence observed could be initially caused by a defect in viral positive-strand RNA synthesis<sup>42</sup>. Despite the very low viral RNA load, viral RNA could still be detected in clusters of infected cardiomyocytes of patients suffering from unexplained DCM (Figure 2)<sup>3,38</sup>. Our results indicated that the cardiac tissue of these 8 EV-positive patients suffering from end-stage idiopathic DCM was infected by persistent EVs.

After validating the persistent infection status of the patient cohort, our study focused on the 5' terminal sequences of persistent viral RNAs. The results showed predominant viral RNA populations harboring 5' terminal deletions in their genomes. These deletions resulted in the loss of stem "a", stem-loop "b," stem-loop "c," and part of stem-loop "d" in the 5' cloverleaf RNA structure (Figure 1B), consistent with results published previously for a fulminant human myocarditis<sup>5</sup> and in a recently published case of EV-induced DCM<sup>9</sup>. These mutations disrupt the host protein PCBP binding site located in stem-loop "b"<sup>43</sup>. However, no deletions within stem-loop "d," near or after the viral protein 3CD binding site, were observed (Figure 3). Moreover, a negative correlation was observed between the proportion of deleted viral RNA populations and viral RNA load (Figure 3D), indicating a potential link between the low viral load characteristic of persistent infection and 5' terminal deletions of EV genomes.

Having established that 5' terminally-deleted forms of EV genomic RNAs were present in cardiac tissues from human DCM patients, we assessed the biological activities of such RNA forms in transfected human primary cardiomyocytes in culture. Results from these experiments revealed major defects in viral RNA replication for the 5' deleted forms of EV RNAs, compared to full-length RNAs or a mixture of deleted forms and full-length RNAs (in a ratio of 19:1, deleted RNA:full-length RNA). Our data are consistent with the results recently reported by Leveque and co-workers<sup>26</sup>, who demonstrated that 5' UTR deletions reduce the binding of replication factors to positive-strand CV-B3 RNA, resulting in non-detectable RNA replication activities in cardiomyocytes or HeLa cells. Since we observed that 20% of DCM samples harbored the viral 5' deleted forms of RNA alone in cardiac tissues (Figure 3), we hypothesize that the viral replication activities of these deleted forms described in Figure 4 could be sustained during long-term chronic human cardiac cell infections in DCM patients. This hypothesis is strongly supported by previous experimental work that identified the persistence of 5' UTR deleted CVB- chronic infections in non-

cardiac human cells or in cardiac or pancreatic tissues of murine models without the presence of detectable full-length RNA forms<sup>5,6,8,44</sup>. It should be noted that in these latter studies by Chapman and co-workers, replication of a 5' 49 nt-deleted CV-B RNA form was detected in both HeLa cells and infected mice.

In an effort to understand how the presence of both full-length and deleted forms of EV genomic RNA in the same tissue might influence viral gene expression and replication functions, we discovered that transfection of a mixture of 5' deleted and full-length CV-B3 RNA forms initially produced higher viral RNA replication activities than those observed with full-length forms alone. In later times after transfection, these mixtures led to reduced levels of viral RNA synthesis compared to those produced by the full-length form alone. We suggest that the full-length viral RNA form could initially provide helper functions to the deleted RNA forms by providing viral proteins involved in replication and by stimulating the synthesis of negative-strand RNA intermediates<sup>5,26</sup>. Subsequently, this could result in a *trans*-dominant negative effect due to formation of RNA replication complexes that are reduced in their capacity to synthesize positive-strand RNAs. Such a scenario would lead to low viral loads and infectious particle levels<sup>6</sup>.

A remaining mechanistic question addressed in our study was how the presence of very low levels of replication-impaired, 5' terminally-deleted forms of EV RNA could mediate cellular pathology. We found that there were no significant differences in the overall translation efficiencies of the different RNA forms, confirming that the 5' terminal viral RNA deletions identified in our study do not interfere with the synthesis of the viral polyprotein. As a result, we turned to the expression of viral protein 2A<sup>pro</sup>, a protein previously implicated in EV cardiac pathogenesis<sup>12,13</sup> and its impact on HCM functions. We used eIF4G cleavage as a biological readout for 2A proteolytic activity, since the detection of the catalytic activity of 2A<sup>pro</sup> allowed for a more sensitive detection of viral replication than direct detection of viral proteins. We observed significantly more viral proteinase activity in HCM transfected by CV-B3 full-length RNAs compared to deleted RNA forms when similar levels of RNA were transfected (Figure 5D). In transfection experiments mimicking the full-length and deleted form proportions observed in patients, the combination of 125 ng of full length and 2,375 ng of d50 RNA induced more eIF4G disruption than the same quantities of d50 RNA alone (refer to Figure 5A). This effect was abolished when using a specific inhibitor of 2A<sup>pro</sup> or a viral RNA harboring a catalytically inactive 2A gene (Figure 5D-F). Interestingly, the production of capsid protein was not detected by Western blot in cells transfected with the deleted RNA form alone, but a small amount was observed in cells transfected with a mixture of full-length and deleted RNA forms (Figure 5A, 5C). This result strongly suggests a functional interaction between the two forms of viral RNA. It has been shown that 2A<sup>pro</sup> activity is responsible for dystrophin disruption during CV-B3 infection<sup>12,13</sup>. Moreover, Barnabei and co-workers reported that the cleavage of dystrophin cannot be compensated by utrophin<sup>14</sup>. In our experimental model, even low levels of 2A<sup>pro</sup> induce readily detectible cleavage of host proteins. Such deleterious effects of CV-B persistent infection could be ongoing for years in patients suffering from DCM. Moreover, viruses harboring 5' terminal RNA deletions can replicate in murine and cellular models<sup>6,8</sup>, and based on the low dose of 2A<sup>pro</sup> needed to disrupt host cell functions, we suggest that these low-level replicating viruses could either be involved directly in DCM

pathogenesis or augment the damages caused during acute infection. We do not exclude other mechanisms that could lead to increased pathogenesis, given that the infection triggers an immune response against the viral genome and viral proteins, inducing apoptosis and immune system activation.

In summary, our results demonstrate that major persistent forms of EV-B 5' deleted genomic RNAs (alone or in association with cooperative viral populations harboring full-length genomic RNAs) are associated with the pathogenesis of unexplained DCM cases, possibly via viral 2A<sup>Pro</sup> proteolytic activity, confirming and significantly extending the work from Knowlton's group and others<sup>45</sup>. These results provide a better understanding of the molecular mechanisms that underlie the persistence of EV forms in human cardiac tissues and should stimulate the development of new therapeutic strategies for acute and chronic cardiac infections, such as DCM, caused by enteroviruses. Based on our results, it seems critical to intensify the search for specific inhibitors of the CV-B 2A<sup>Pro</sup> activity, especially since some progress has already been made on this front<sup>46</sup>. Inhibition of 2A proteinase activity might be expected to act on two levels by (i) preventing the maturation of viral polyproteins, and thus viral replication, and (ii) inhibiting the shut off of host cell translation as well as the disruption of dystrophin and its crucial functions in the cell.

## Supplementary Material

Refer to Web version on PubMed Central for supplementary material.

## Acknowledgments:

We thank Maxime Hentzien for his skillful assistance in statistical analyses. We thank Christine Terryn (PICT-IBISA platform, URCA Reims) for her skillful assistance and her expertise in confocal microscopy analyses. We thank Alain Rico and Stephane Jankowsky (Life Technology, Paris, France) for their expertise and skillful assistance on the NGS ion Torrent sequencing protocol and analyses of the NGS data.

### Source of Funding

Alexis Bouin was supported by a MESR PhD grant from the French research ministry and by a postdoctoral fellowship from the George E. Hewitt Foundation for Medical Research. Nicolas Lévêque was supported by a Marie Curie International Outgoing Fellowship for Career Development from the European Commission (contract no. 622308) and by grants from the Philippe Foundation and the Champagne-Ardenne region. This work was funded, in part, by 2015–2017 grants for Clinical and Virological Research (IFR53/EA-4684) from the Medical University and School of Medicine of Reims, France, by the Grog Chard Foundation, and by U.S. Public Health Service grants AI022693 and AI026765 from the National Institutes of Health.

## References

1. Racaniello VR. Picornaviridae: The viruses and Their Replication In: Fields Virology. New York: Knipe & Howley; 2007 p. 795–838.
2. Dennert R, Crijns HJ, Heymans S. Acute viral myocarditis. *Eur Heart J.* 2008;29:2073–2082. [PubMed: 18617482]
3. Li Y, Bourlet T, Andreoletti L, Mosnier JF, Peng T, Yang Y, Archard LC, Pozzetto B, Zhang H. Enteroviral capsid protein VP1 is present in myocardial tissues from some patients with myocarditis or dilated cardiomyopathy. *Circulation.* 2000;101:231–234. [PubMed: 10645916]
4. Nguyen Y, Renois F, Leveque N, Giusti D, Picard-Maureau M, Bruneval P, Fornes P, Andreoletti L. Virus detection and semiquantitation in explanted heart tissues of idiopathic dilated cardiomyopathy adult patients by use of PCR coupled with mass spectrometry analysis. *J Clin Microbiol.* 2013;51:2288–2294. [PubMed: 23658274]



5. Chapman NM, Kim K-S, Drescher KM, Oka K, Tracy S. 5' terminal deletions in the genome of a coxsackievirus B2 strain occurred naturally in human heart. *Virology*. 2008;375:480–491. [PubMed: 18378272]
6. Kim K-S, Tracy S, Tappich W, Bailey J, Lee C-K, Kim K, Barry WH, Chapman NM. 5'-Terminal deletions occur in coxsackievirus B3 during replication in murine hearts and cardiac myocyte cultures and correlate with encapsidation of negative-strand viral RNA. *J Virol*. 2005;79:7024–7041. [PubMed: 15890942]
7. Vogt DA, Andino R. An RNA element at the 5'-end of the poliovirus genome functions as a general promoter for RNA synthesis. *PLoS Pathog*. 2010;6:e1000936. [PubMed: 20532207]
8. Jaramillo L, Smithee S, Tracy S, Chapman NM. Domain I of the 5' non-translated genomic region in coxsackievirus B3 RNA is not required for productive replication. *Virology*. 2016;496:127–130. [PubMed: 27289561]
9. Bouin A, Nguyen Y, Wehbe M, Renois F, Fornes P, Bani-Sadr F, Metz D, Andreoletti L. Major Persistent 5' Terminally Deleted Coxsackievirus B3 Populations in Human Endomyocardial Tissues. *Emerg Infect Dis*. 2016;22:1488–1490. [PubMed: 27434549]
10. Bordería AV, Isakov O, Moratorio G, Henningsson R, Agüera-González S, Organtini L, Gnädig NF, Blanc H, Alcover A, Hafenstein S, Fontes M, Shomron N, Vignuzzi M. Group Selection and Contribution of Minority Variants during Virus Adaptation Determines Virus Fitness and Phenotype. *PLOS Pathog*. 2015;11:e1004838. [PubMed: 25941809]
11. Collis PS, O'Donnell BJ, Barton DJ, Rogers JA, Flanagan JB. Replication of poliovirus RNA and subgenomic RNA transcripts in transfected cells. *J Virol*. 1992;66:6480–6488. [PubMed: 1328676]
12. Badorff C, Lee GH, Lamphear BJ, Martone ME, Campbell KP, Rhoads RE, Knowlton KU. Enteroviral protease 2A cleaves dystrophin: evidence of cytoskeletal disruption in an acquired cardiomyopathy. *Nat Med*. 1999;5:320–326. [PubMed: 10086389]
13. Xiong D, Yajima T, Lim B-K, Stenbit A, Dublin A, Dalton ND, Summers-Torres D, Molkentin JD, Duplain H, Wessely R, Chen J, Knowlton KU. Inducible cardiac-restricted expression of enteroviral protease 2A is sufficient to induce dilated cardiomyopathy. *Circulation*. 2007;115:94–102. [PubMed: 17190866]
14. Barnabei MS, Sjaastad FV, Townsend D, Bedada FB, Metzger JM. Severe dystrophic cardiomyopathy caused by the enteroviral protease 2A-mediated C-terminal dystrophin cleavage fragment. *Sci Transl Med*. 2015;7:294ra106.
15. Elliott P, Andersson B, Arbustini E, Bilinska Z, Cecchi F, Charron P, Dubourg O, Kühl U, Maisch B, McKenna WJ, Monserrat L, Pankuweit S, Rapezzi C, Seferovic P, Tavazzi L, Keren A. Classification of the cardiomyopathies: a position statement from the European Society Of Cardiology Working Group on Myocardial and Pericardial Diseases. *Eur Heart J*. 2008;29:270–276. [PubMed: 17916581]
16. N'Guyen Y, Lesaffre F, Metz D, Tassan S, Saade Y, Boulagnon C, Fornes P, Renois F, Andreoletti L. Enterovirus but not Parvovirus B19 is associated with idiopathic dilated cardiomyopathy and endomyocardial CD3, CD68, or HLA-DR expression: Virus & Inflammatory Marker Detection in DCM. *J Med Virol*. 2017;89:55–63. [PubMed: 27301802]
17. Carrick DM, Mehaffey MG, Sachs MC, Altekruse S, Camalier C, Chuaqui R, Cozen W, Das B, Hernandez BY, Lih C-J, others. Robustness of next generation sequencing on older formalin-fixed paraffin-embedded tissue. *PloS One*. 2015;10:e0127353. [PubMed: 26222067]
18. Tu Z, Chapman NM, Hufnagel G, Tracy S, Romero JR, Barry WH, Zhao L, Currey K, Shapiro B. The cardiovirulent phenotype of coxsackievirus B3 is determined at a single site in the genomic 5' nontranslated region. *J Virol*. 1995;69:4607–4618. [PubMed: 7609025]
19. Martin U, Jarasch N, Nestler M, Rassmann A, Munder T, Seitz S, Zell R, Wutzler P, Henke A. Antiviral effects of pan-caspase inhibitors on the replication of coxsackievirus B3. *Apoptosis Int J Program Cell Death*. 2007;12:525–533.
20. Marissen WE, Lloyd RE. Eukaryotic translation initiation factor 4G is targeted for proteolytic cleavage by caspase 3 during inhibition of translation in apoptotic cells. *Mol Cell Biol*. 1998;18:7565–7574. [PubMed: 9819442]
21. Yu SF, Lloyd RE. Identification of essential amino acid residues in the functional activity of poliovirus 2A protease. *Virology*. 1991;182:615–625. [PubMed: 1850921]



22. Tershak DR. Inhibition of poliovirus polymerase by guanidine in vitro. *J Virol.* 1982;41:313–318. [PubMed: 6283124]
23. Zuo J, Quinn KK, Kye S, Cooper P, Damoiseaux R, Krogstad P. Fluoxetine Is a Potent Inhibitor of Coxsackievirus Replication. *Antimicrob Agents Chemother.* 2012;56:4838–4844. [PubMed: 22751539]
24. Leveque N, Van Haecke A, Renois F, Boutolleau D, Talmud D, Andreoletti L. Rapid virological diagnosis of central nervous system infections by use of a multiplex reverse transcription-PCR DNA microarray. *J Clin Microbiol.* 2011;49:3874–3879. [PubMed: 21918017]
25. Walter BL, Parsley TB, Ehrenfeld E, Semler BL. Distinct poly(rC) binding protein KH domain determinants for poliovirus translation initiation and viral RNA replication. *J Virol.* 2002;76:12008–12022. [PubMed: 12414943]
26. Lévêque N, Garcia M, Bouin A, Nguyen JHC, Tran GP, Andreoletti L, Semler BL. Functional Consequences of RNA 5′-Terminal Deletions on Coxsackievirus B3 RNA Replication and Ribonucleoprotein Complex Formation. *J Virol.* 2017;91:e00423–17. [PubMed: 28539455]
27. Bock C-T, Klingel K, Kandolf R. Human parvovirus B19-associated myocarditis. *N Engl J Med.* 2010;362:1248–1249. [PubMed: 20357294]
28. Leveque N, Renois F, Talmud D, Nguyen Y, Lesaffre F, Boulagnon C, Bruneval P, Fornes P, Andreoletti L. Quantitative Genomic and Antigenomic Enterovirus RNA Detection in Explanted Heart Tissue Samples from Patients with End-Stage Idiopathic Dilated Cardiomyopathy. *J Clin Microbiol.* 2012;50:3378–3380. [PubMed: 22837323]
29. Giachetti C, Semler BL. Role of a viral membrane polypeptide in strand-specific initiation of poliovirus RNA synthesis. *J Virol.* 1991;65:2647–2654. [PubMed: 1850038]
30. Novak JE, Kirkegaard K. Improved method for detecting poliovirus negative strands used to demonstrate specificity of positive-strand encapsidation and the ratio of positive to negative strands in infected cells. *J Virol.* 1991;65:3384–3387. [PubMed: 1851886]
31. Lloyd RE. Translational control by viral proteinases. *Virus Res.* 2006;119:76–88. [PubMed: 16303201]
32. Chase AJ, Semler BL. Viral subversion of host functions for picornavirus translation and RNA replication. *Future Virol.* 2012;7:179–191. [PubMed: 23293659]
33. Tracy S, Drescher KM, Chapman NM. Enteroviruses and type 1 diabetes. *Diabetes Metab Res Rev.* 2011;27:820–823. [PubMed: 22069266]
34. Andréoletti L, Lévêque N, Boulagnon C, Brasselet C, Fornes P. Viral causes of human myocarditis. *Arch Cardiovasc Dis.* 2009;102:559–568. [PubMed: 19664576]
35. Bowles NE, Richardson PJ, Olsen EG, Archard LC. Detection of Coxsackie-B-virus-specific RNA sequences in myocardial biopsy samples from patients with myocarditis and dilated cardiomyopathy. *Lancet.* 1986;1:1120–1123. [PubMed: 2871380]
36. Fairweather D, Stafford KA, Sung YK. Update on coxsackievirus B3 myocarditis. *Curr Opin Rheumatol.* 2012;24:401–407. [PubMed: 22488075]
37. Cooper LT Jr. Myocarditis. *N Engl J Med.* 2009;360:1526–1538. [PubMed: 19357408]
38. Andreoletti L, Wattré P, Decoene C, Lobert PE, Dewilde A, Hober D. Detection of enterovirus-specific RNA sequences in explanted myocardium specimens from patients with dilated or ischemic cardiomyopathy. *Clin Infect Dis Off Publ Infect Dis Soc Am.* 1995;21:1315–1317.
39. Oldstone MBA. Viral persistence: parameters, mechanisms and future predictions. *Virology.* 2006;344:111–118. [PubMed: 16364742]
40. Cunningham L, Bowles NE, Lane RJM, Dubowitz V, Archard LC. Persistence of enteroviral RNA in chronic fatigue syndrome is associated with the abnormal production of equal amounts of positive and negative strands of enteroviral RNA. *J Gen Virol.* 1990;71:1399–1402. [PubMed: 2161907]
41. Ertel KJ, Brunner JE, Semler BL. Mechanistic consequences of hnRNP C binding to both RNA termini of poliovirus negative-strand RNA intermediates. *J Virol.* 2010;84:4229–4242. [PubMed: 20164237]
42. Sharma N, Ogram SA, Morasco BJ, Spear A, Chapman NM, Flanagan JB. Functional role of the 5′terminal cloverleaf in Coxsackievirus RNA replication. *Virology.* 2009;393:238–249. [PubMed: 19732932]

43. Parsley TB, Towner JS, Blyn LB, Ehrenfeld E, Semler BL. Poly (rC) binding protein 2 forms a ternary complex with the 5'-terminal sequences of poliovirus RNA and the viral 3CD proteinase. *RNA N Y N*. 1997;3:1124–1134.
44. Kim K-S, Chapman NM, Tracy S. Replication of coxsackievirus B3 in primary cell cultures generates novel viral genome deletions. *J Virol*. 2008;82:2033–2037. [PubMed: 18057248]
45. Lim B-K, Peter AK, Xiong D, Narezkina A, Yung A, Dalton ND, Hwang K-K, Yajima T, Chen J, Knowlton KU. Inhibition of Cocksackievirus-associated dystrophin cleavage prevents cardiomyopathy. *J Clin Invest*. 2013;123:5146–5151. [PubMed: 24200690]
46. Maghsoudi N, Tafreshi NK, Khodagholi F, Zakeri Z, Esfandiarei M, Hadi-Alijanvand H, Sabbaghian M, Maghsoudi AH, Sajadi M, Zohri M, Moosavi M, Zeinoddini M. Targeting enteroviral 2A protease by a 16-mer synthetic peptide: inhibition of 2Apro-induced apoptosis in a stable Tet-on HeLa cell line. *Virology*. 2010;399:39–45. [PubMed: 20096913]

## Clinical Perspective

### What is new?

- We performed deep sequencing of viral RNA from cardiac tissue of patients with enterovirus (EV) related end-stage dilated cardiomyopathy (DCM) and then transfected viral RNA clones mimicking the viral genomes found in patient tissues into primary human cardiac cells to assess their replication activities and impact on cardiomyocyte functions.
- Our findings demonstrated that the major persistent viral forms are composed of B-type enteroviruses harboring a 5' terminal deletion (17 to 50 nucleotides) in their genomic RNAs.
- These viruses alone or associated with full-length populations of helper RNAs could impair cardiomyocyte functions by viral 2A<sup>PRO</sup> activities in EV-DCM cases.

### What are the clinical implications?

- In EV induced-dilated cardiomyopathy (DCM) cases (33% of idiopathic DCM cases), only symptomatic treatments against the failure of cardiac functions are available.
- Based on our results, it seems critical to develop specific inhibitors of the EV-2A<sup>PRO</sup> activity that might prevent viral replication and inhibit the shut-off of host cell translation as well as the disruption of dystrophin.
- In early-diagnosed EV induced DCM cases, the use of such protease inhibitors could efficiently decrease and stop the chronic pathophysiological process of DCM and therefore reduce the need for heart transplantation at the end-stage of this chronic cardiomyopathy.



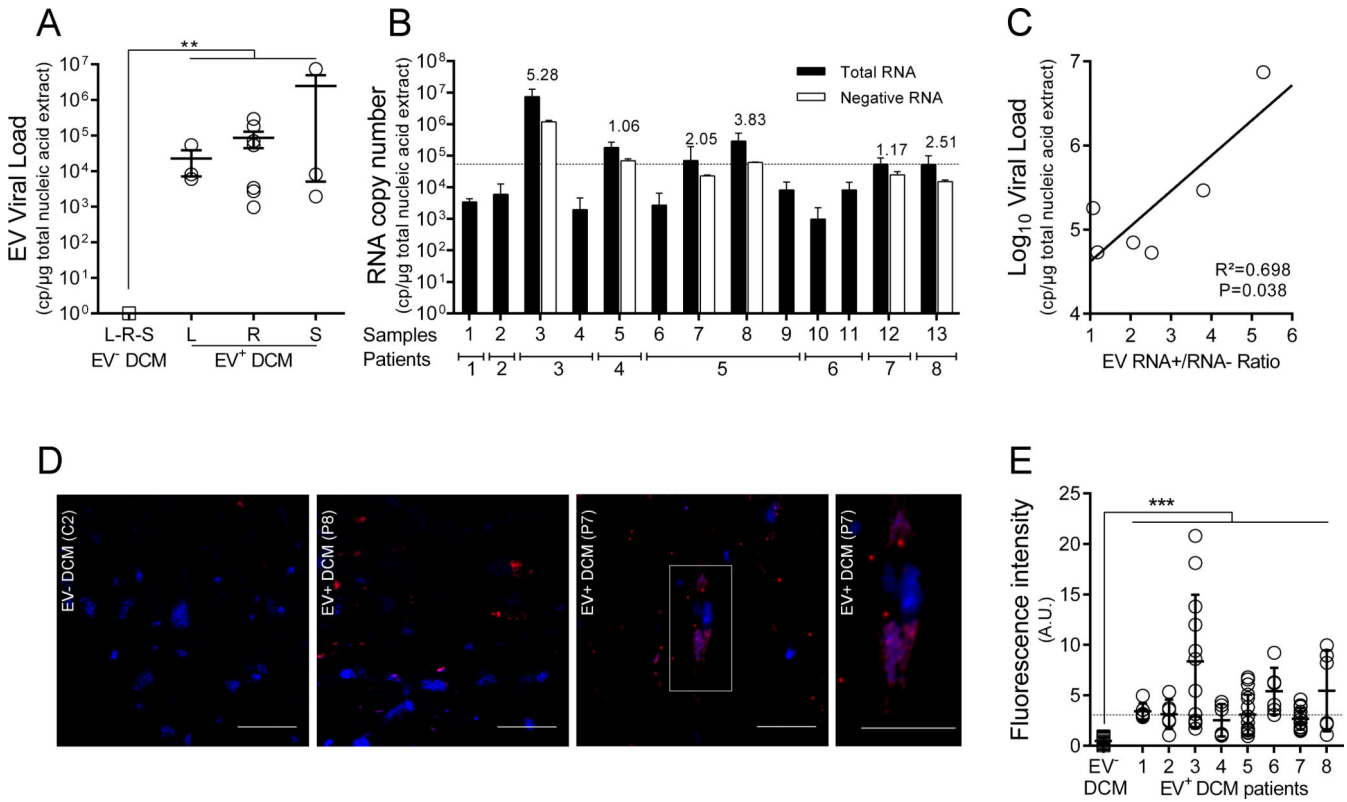


**Figure 2. Detection and characterization of EV persistent infection in cardiac tissues of idiopathic DCM patients.**

**A.** Total EV RNA levels (copies/ $\mu\text{g}$  of total nucleic acid extract) in cardiac tissues of EV positive IDCM patients (8 of 24 tested IDCM patients) and healthy controls ( $n=14$ ) were quantified using a generic EV RT-qPCR. Dots represent patients mean values ( $n=8$ ). L: Left Ventricle, R: Right Ventricle, S: Septum. \*\*:  $P<0.01$  by Mann-Whitney U test. **B.** Quantification (RT-qPCR) of total and minus EV RNA strands in tissues of 8 EV positive IDCM patients ( $n=13$  samples) using specific primers to each RNA strand polarity. Data represent mean values  $\pm$  SEM ( $n=13$ ); RNA+/RNA- ratio values are indicated as an index above each sample. When RNA minus strand levels were below the threshold of quantification value, RNA+/RNA- ratios were not calculated. **C.** Linear regression curve between the  $\log_{10}$  genome copies/ $\mu\text{g}$  and RNA+/RNA- ratio values ( $n=6$ ) ( $P=0.038$ ;  $R^2=0.70$ ). **D.** *In situ* Hybridization (ISH) targeting viral RNA (upper panels) displaying EV RNA (red) in serial cardiac tissue sections of infected DCM. Nuclei are stained in blue; Bar scale = 50  $\mu\text{m}$ . White square (DCM+ EV+) corresponds to a high magnification (X400) of a single EV positive cardiomyocytes (bar scale = 50  $\mu\text{m}$ ). **E.** Fluorescence signal due to *in situ* hybridization of viral RNA observed in each slide was quantitatively estimated using Image J software (Software free NIH) three times at two magnifications (X20 and X40). Briefly, thresholding techniques were successively performed to remove background noise and empty spaces and to select relevant fluorescent cytoplasmic foci due to *in situ* hybridization. Results were expressed as fluorescent pixels per 100,000. \*\*\*:  $P<0.001$  by Mann Whitney U test.

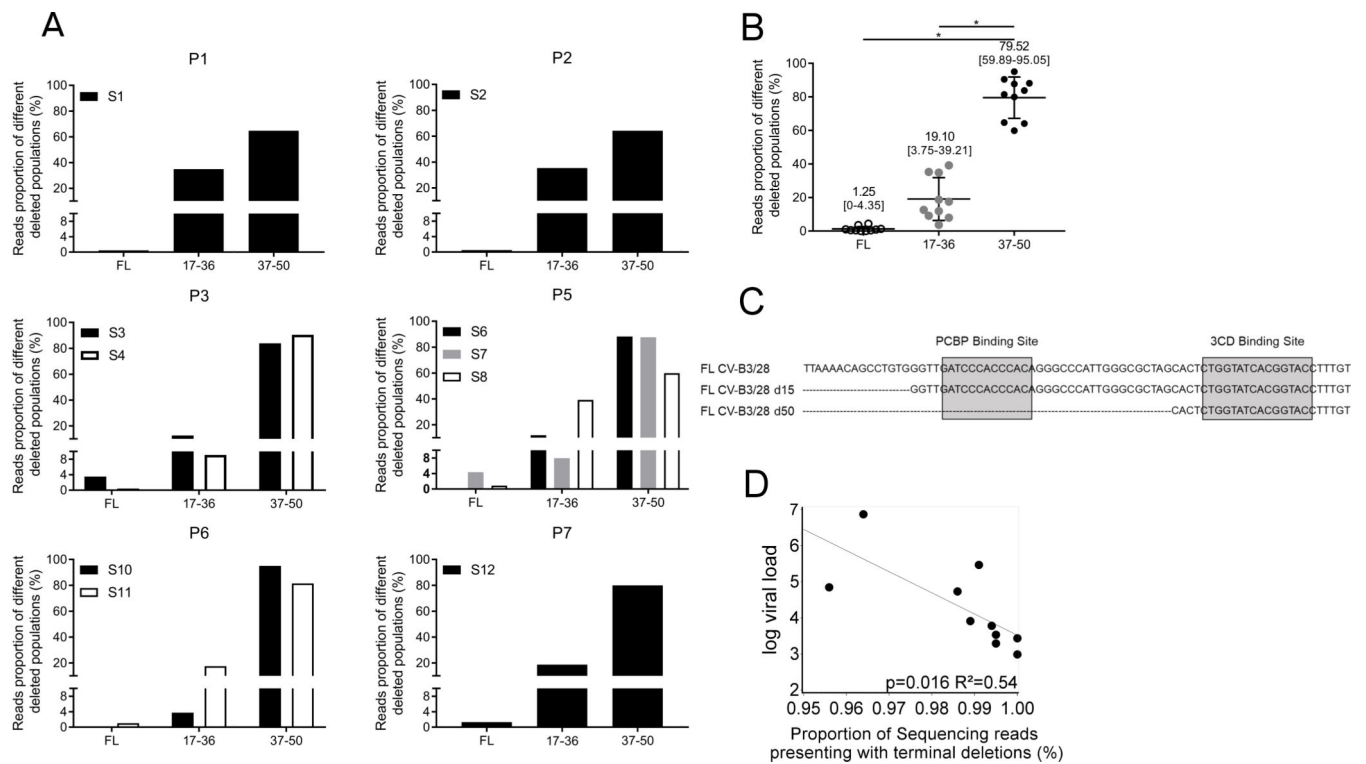


**Figure 3. Characterization of persistent 5' terminal deleted EV populations**

**A.** Proportion of sequence reads detected in each patient (n=7) for each group of viral forms: Full-length (FL), deleted from 17 to 36 nucleotides (17–36) and deleted from 37 to 50 nucleotides (37–50). If multiple samples were obtained from a patient, they are displayed independently. **B.** Proportion of sequence reads found in the whole cohort for Full Length (FL) viruses and deleted forms groups of 17–36 and 37–50 nucleotides. Black bars represent the mean values [min., max. values]. \* $P < 0.001$  by Mann-Whitney U test. **C.** Schematic representation of the 5' terminal deletions of EV-B cloverleaf structure with its binding sites for host PCBP and viral 3CD proteins. **D.** Linear regression curve between the  $\log_{10}$  EV genome copies/ $\mu\text{g}$  and reads proportion of deleted forms (both 17–36 and 37–50 groups) in each sample (n=10) indicating a decrease in the viral load when proportion of deleted forms increased ( $R^2=0.54$ ;  $P=0.016$ ).

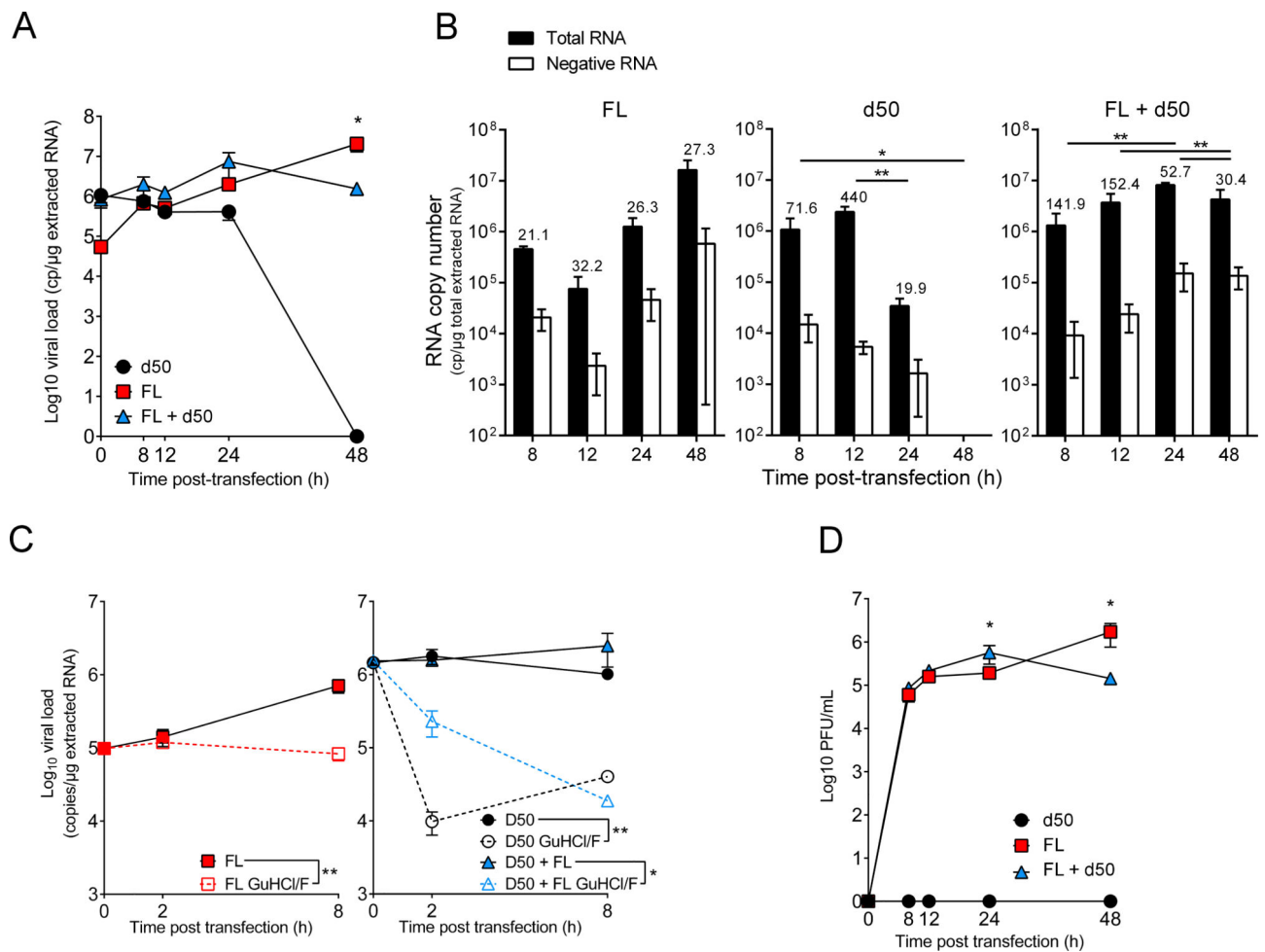


**Figure 4. Analysis of early and late replication activities of 5' terminally deleted, full-length, and mixed CV-B3/28 RNA populations in primary human cardiac cells.**

**A–C.** Synthetic RNAs (100 ng) of full-length (red squares) or deleted of 50 5' terminal nucleotides (black circles) of CV-B3/28 forms were transfected alone or in association (95% of d50 associated with 5% of FL, blue triangles) in primary human cardiomyocytes (HCM): **A.** Viral RNA genomic replication activity (total viral RNA (intra and extracellular production)) was assessed using a RT-qPCR assay at 0, 8, 12, 24 and 48 hr post transfection. Data represent the mean ± SEM. \*: P < 0.05 by Mann Whitney U test (n=3). **B.** Quantification by RT-qPCR of total, minus and EV RNA plus and minus strand ratios at each time post-transfection (in hours). RNA+/RNA- ratio values are indicated as an index above each sample. Data represent the mean ± SEM. Statistical analysis were assessed on the RNA+/RNA- ratios, \*: P < 0.05; \*\*: P < 0.01 by Mann Whitney U test (n=3). **C.** Viral RNA replication inhibition assay using guanidine hydrochloride (GuHCl; 2 mM) and fluoxetine (F; 8 μM) was performed at 0, 2 and 8 hr (h) post transfection for each viral form (d50: empty circle, FL: empty square, and mixed d50 + FL: empty triangle). Data represent the mean ± SEM. \*: P < 0.05; \*\*: P < 0.01; according to repeated measures two-way ANOVA test. **D.** Analysis of intra- and extra-cellular infectious particle production at 0, 8, 12, 24 and 48 hr (h) post transfection (n=3). Data represent the mean ± SEM. \*: P < 0.05 by Mann Whitney U test.



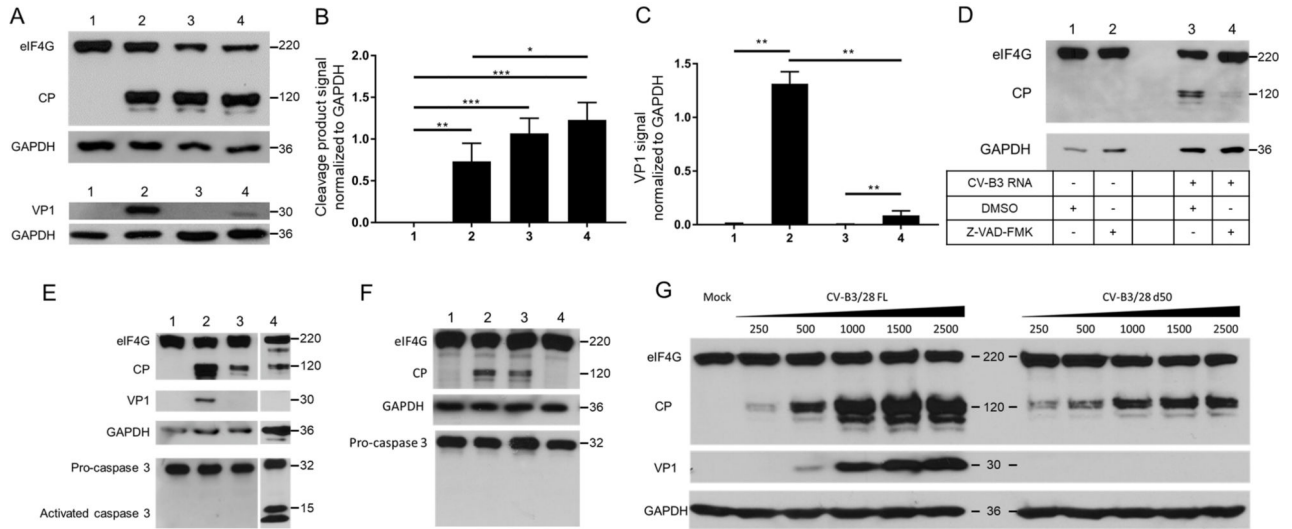


**Figure 5. Viral protein production and analysis of 2A<sup>Pro</sup> activity in CV-B3 transfected human cardiomyocytes.**

**A.** Western blot assay detecting eIF4G and VP1 in human cardiomyocytes at 24 hr post transfection of CV-B3/28 FL RNA, CV-B3/28 d50 RNA and both forms together. Proteins were subjected to electrophoresis on an SDS-containing polyacrylamide gel. 1: Mock transfected, 2: 125 ng CV-B3/28 FL, 3: 2375 ng CV-B3/28 d50, 4: 125 ng CV-B3/28 FL + 2375 ng CV-B3/28 d50. **B.** Signals detected for eIF4G cleavage fragment in Western blot were standardized using GAPDH and quantified. 1: Mock transfected, 2: 125 ng CV-B3/28 FL, 3: 2375 ng CV-B3/28 d50, 4: 125 ng CV-B3/28 FL + 2375 ng CV-B3/28 d50. VP1 signal standardized with total eIF4G detection. **C.** Signals detected for VP1 in Western blot were standardized using GAPDH and quantified. 1: Mock transfected, 2: 125 ng CV-B3/28 FL, 3: 2375 ng CV-B3/28 d50, 4: 125 ng CV-B3/28 FL + 2375 ng CV-B3/28 d50. **D.** Western blot assay detecting eIF4G and VP1 in human cardiomyocytes at 12 hr post transfection of CV-B3/28 FL RNA. Z-VAD-FMK is reported to inhibit CV-B3 2A<sup>Pro</sup>. Synthetic full length (FL) CV-B3/28 RNA was transfected in HCM and proteins were extracted at 24 hr. Proteins were subjected to electrophoresis on an SDS-containing polyacrylamide gel. **E.** Detection of caspase-3 activation: Western blot assay detecting eIF4G and VP1 and caspase-3 in human cardiomyocytes at 24 hr post transfection. Proteins were subjected to electrophoresis on an SDS-containing polyacrylamide gel. 1: Mock; 2: CV-B3/28 FL; 3: CV-B3/28 d50; 4: Staurosporin treated. **F.** Western blot assay targeting eIF4G and caspase-3 in human cardiomyocytes at 24 hr post transfection. Proteins were subjected to electrophoresis on an SDS-containing polyacrylamide gel. 1: Mock; 2: CV-B3/28 FL; 3: CV-B3/28 d50; 4: CV-B2/28 FL C107S. **G.** Western blot assay detecting eIF4G and VP1 in human cardiomyocytes at 24 hr post transfection of CV-B3/28 FL RNA or CV-B3/28 d50 RNA. Amounts of transfected RNA are indicated above lanes. Proteins were subjected to electrophoresis on an SDS-containing polyacrylamide gel. \*: P<0.05; \*\*: P<0.01, \*\*\*: P<0.001. Apparent molecular weights are indicated on the right side of Western blot images.